Eur. Phys. J. D **14**, 119–125 (2001)

THE EUROPEAN PHYSICAL JOURNAL D

EDP Sciences

Effective quantum efficiency in the pulsed homodyne detection of a n-photon state

F. Grosshans and P. Grangier[a]

Laboratoire Charles Fabry, Institut d'Optique Théorique et Appliquée, 91403 Orsay, France

Received 27 July 2000 and Received in final form 29 November 2000

Abstract. Homodyne detection can be used to perform measurements on various quantum states of the light, such as conditional single photon states produced by parametric fluorescence processes. In the pulsed regime, the time and frequency overlap between the single photon wave packet and the local oscillator field plays a crucial role. We show in this paper that this overlap can be characterized by an effective quantum efficiency, which is explicitly calculated in various situations of experimental interest.

PACS. 42.50.Dv Nonclassical field states; squeezed, antibunched, and sub-Poissonian states; operational definitions of the phase of the field; phase measurements – 42.50.Ar Photon statistics and coherence theory – 42.65.Re Ultrafast processes; optical pulse generation and pulse compression

1 Introduction

Photon number states (Fock states) play a fundamental role in quantum optics, both from a conceptual point of view — because number states provide the most convenient basis for the states of the quantized electromagnetic field [1] — and from an experimental point of view — because the generation and detection of number states provide one of the the most striking evidence for the quantum nature of the light [2,3]. Beyond these fundamental issues, it has also been realized that single photon states (*i.e.* photon number states with $n = 1$) also play a central role in quantum information processing: a one-photon, two-mode state of the field is the simplest implementation of a "qubit", and it has been exploited with great success as the basic tool for quantum cryptography [4].

The usual way to detect a single photon state is by photon counting, *i.e.* by photo-emission in a photocathode or a semiconductor medium, followed by strong amplification based upon an avalanche process. The specific quantum properties of a single photon state can then be evidenced by measuring correlation between several photodetection events. Generation of approximate single-photon states, obtained by controlling the emission of the source at the single photon level, may yield "antibunching" [5,6] or "anticorrelation" [3] effects. However, this direct detection method does not give access to the full properties of a Fock states, which by analogy with a mechanical oscillator can also be observed in the "position and momentum" eigenbasis, and not only in the energy (photon number) eigenbasis which is associated to photon counting. For the electromagnetic field, the equivalent of the position and momentum eigenbasis correspond to the quadrature amplitudes of the electric field, and can be measured by using homodyne detection.

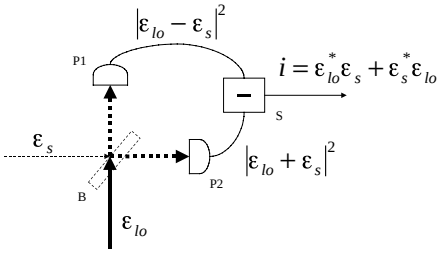

Fig. 1. Homodyne detector. In a balanced homodyne detector, the weak field $\mathcal{E}_\mathrm{s}$ to be measured interferes on a balanced beam splitter B with a strong local-oscillator $\mathcal{E}_\mathrm{lo}$ of same frequency. The optical intensities of the two output ports of the beam splitter are measured with the photodetectors P1 and P2 and substracted by the power combiner S. The output current i of the detector is then proportional to $\mathcal{E}_\mathrm{lo}^* \mathcal{E}_\mathrm{s} + \mathcal{E}_\mathrm{s}^* \mathcal{E}_\mathrm{lo}$.

In a balanced homodyne detector (see Fig. 1), the weak field $\mathcal{E}_\mathrm{s}$ to be measured interferes on a balanced beam splitter with a strong local-oscillator $\mathcal{E}_\mathrm{lo}$ of same frequency. The output current of the detector is proportional to the difference between the optical intensities of the two output ports of the beam splitter. Since these intensities are proportional to $|\mathcal{E}_\mathrm{lo} \pm \mathcal{E}_\mathrm{s}|^2$, their difference is proportional to $\mathcal{E}_\mathrm{lo}^* \mathcal{E}_\mathrm{s} + \mathcal{E}_\mathrm{s}^* \mathcal{E}_\mathrm{lo}$. The weak field $\mathcal{E}_\mathrm{s}$ is thus multiplied by the strong local-oscillator field $\mathcal{E}_\mathrm{lo}$, and the choice of the relative phase between these two fields gives access to the various quadrature amplitudes of the signal field.

In 1987, Yurke and Stoler proposed to perform an homodyne measurement of a conditional single photon state [7]. The production of such a state is based upon the production of pairs of photon by spontaneous atomic [3]

[a] e-mail: philippe.grangier@iota.u-psud.fr

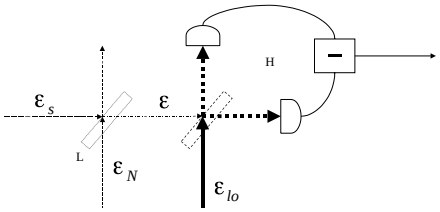

Fig. 2. Imperfect homodyne detector. An imperfect homodyne detector of quantum efficiency η is simulated with a beam-splitter L in the input port of a perfect homodyne detector H, mixing the field to measure $\mathcal{E}_{\rm s}$ with vacuum $\mathcal{E}_{\rm N}$. Its transmission coefficient t verifies $|t|^2 = \eta$.

or parametric [2] fluorescence. The detection of one photon then projects the field in a single photon state, which can then be detected by various methods. In the scheme of reference [7], the second photon of the pair interferes with a local oscillator (L.O.) in an homodyne detection set-up. The measured quantity is then a quadrature amplitude of the electric field, and its probability density should be the same as the one of a mechanical oscillator in position space. In particular, if the state measured is a n-photon Fock state, this probability distribution will exhibit $n+1$ peaks and n zeros (or dark fringes) [10]. These features do not depend on the phase setting of the homodyne detector, due to the phase-independency of the n-photon Fock state.

However, several difficulties prevented this experiment to be completed up to now [8]. First, it was pointed out by Yurke and Stoler that the shape of the probability density is extremely sensitive to the overall quantum efficiency of the homodyne detection set-up, and that the visibility of the fringes decreases quickly with the quantum efficiency η of the detector. For instance, in order to separate the two peaks of a single photon Fock state, a detection system with a high enough global quantum efficiency ($\eta > 1/3$) is needed.

Second, Yurke and Stoler's approach was a single mode calculation, which did not consider in great detail the necessary "time *vs.* frequency" aspect of this experiment. Using hand-waving arguments, it is clear that the single photon state must be prepared in modes which overlap perfectly the L.O. mode, both in time and in frequency: if the timing is wrong, the homodyne detection will see vacuum modes rather than the expected single photon state; if the frequency is wrong, the beat note in the signal-L.O. interference will average to zero. Moreover, time and frequency are not independent due to the Fourier transforms (or time-energy Heisenberg relations) which relate time and energy. An approach to these problems was provided in reference [9], and the measurement result which can be expected in a given experiment was computed explicitly. In the present paper, we will use another approach, which gives essentially the same results, but with a different physical picture: our goal is to hide the time-frequency aspect of this problem under an "effective quantum efficiency" $\eta_{\rm eff}$, and to give a convenient formula for evaluating $\eta_{\rm eff}$ for practical situations of interest. The advantage of our approach is to provide a "translation" between the simple single-mode model of reference [7], and a more realistic experimental situation involving time-dependent signals. This method will be applied to a few simple examples, which include the original Yurke and Stoler's scheme, as well as some more realistic conditions for parametric fluorescence under pulsed laser excitation.

2 Effective efficiency of a pulsed homodyne detector

2.1 Introduction

The main purpose of the calculation presented now is to link the parameters of an imperfect single-mode homodyne detector with the parameters of a pulsed homodyne detector, in order to have the same probability distribution for the detector observables when n-photon Fock states are measured. In the single mode case analyzed in reference [7], the non-unity quantum efficiency of the homodyne detector is modelized by using a beam-splitter which mixes the input field mode s with an empty mode v (see Fig. 2). The transmission and reflection coefficients t and r of the beam-splitter verify $|t|^2 \equiv \eta$ and $|t|^2 + |r|^2 = 1$. The field measured by such a detector is then

$$\hat{a} = t\hat{a}_{\rm s} + r\hat{a}_{\rm v} \tag{1}$$

where the $\hat{a}$ are usual bosonic operators for the various field modes. In the following, the following notations will be used. When the two homodyne detectors are compared, the expression corresponding to the imperfect homodyne detector is written on the left and the one corresponding to the pulsed homodyne detector on the right, the arrow symbolizing a formal analogy between them:

$$\textit{monomode imperfect homodyne detector} \Longleftrightarrow \textit{pulsed perfect homodyne detector.} \tag{2}$$

The definition of the Fourier transform is:

$$\xi(t) = \int {\rm d}\omega\, \xi[\omega] {\rm e}^{{\rm i}\omega t} \text{ and } \xi[\omega] = \frac{1}{2\pi}\int {\rm d}t\, \xi(t) {\rm e}^{-{\rm i}\omega t} \tag{3}$$

and the scalar product is noted with Dirac's formalism:

$$\langle \xi | \mathcal{E} \rangle = \int {\rm d}t\, \xi^*(t)\mathcal{E}(t) = \int {\rm d}\omega {\rm d}t\, \xi^*(t){\rm e}^{{\rm i}\omega t}\mathcal{E}[\omega] = 2\pi \int {\rm d}\omega\, \xi^*[\omega]\mathcal{E}[\omega]. \tag{4}$$

The field states and the measurement operator are defined in Section 2.2. A formal analogy for Fock-states between the two models is found in Section 2.3 and is generalized to more generic field states and imperfect detectors in Section 2.4.

2.2 Input field state and measurement operators

2.2.1 Input field state

In order to compare a Fock state $|n\rangle$ of the monomode field to the correspondent n-photon wave packet $|\psi_n\rangle$, we look for the "wave-packet annihilation operator" $\hat{A}_\mathrm{s}$, analog to the monomode input channel annihilation operator $\hat{a}_\mathrm{s}$. It should verify

$$|n\rangle = \frac{\hat{a}_\mathrm{s}^{\dagger n}}{\sqrt{n!}}|0\rangle \Longleftrightarrow |\psi_n\rangle = \frac{\hat{A}_\mathrm{s}^{\dagger n}}{\sqrt{n!}}|0\rangle, \tag{5}$$

$|0\rangle$ being the vacuum state of the field in both case.

Since the field operator of the input channel of the pulsed homodyne detector is $\hat{E}(t) = \int \mathrm{d}\omega\, \mathrm{e}^{\mathrm{i}\omega t}\hat{a}_\omega$, we can assume

$$\hat{a}_\mathrm{s}^\dagger \Longleftrightarrow \hat{A}_\mathrm{s}^\dagger = \frac{\int \mathrm{d}t\, \xi(t)\hat{E}^\dagger(t)}{\sqrt{2\pi\langle\xi|\xi\rangle}} = \sqrt{\frac{2\pi}{\langle\xi|\xi\rangle}}\int \mathrm{d}\omega\, \xi[\omega]\hat{a}_\omega^\dagger, \tag{6}$$

the function ξ defining the wave packet envelope. The $\sqrt{2\pi/\langle\xi|\xi\rangle}$ prefactor is needed to fulfill the standard commutation relation $[\hat{A}_\mathrm{s}, \hat{A}_\mathrm{s}^\dagger] = 1$.

2.2.2 Homodyne measurement operators

In both homodyne detectors, the local oscillator field $\mathcal{E}_\mathrm{lo}$ will be quasi-classical and much greater than the measured field ($\langle\mathcal{E}_\mathrm{lo}\rangle \gg \langle\hat{a}^\dagger\hat{a}\rangle^{1/2}$ or $\langle\hat{E}^\dagger\hat{E}\rangle^{1/2}$) and therefore assumed to be classical, *i.e.* defined by a complex number commuting with itself. The imperfect monomode homodyne detector is modelized by a perfect detector measuring a mixture of the input mode and an empty mode, as defined by equation (1).

The local oscillator field of the pulsed homodyne detector, $\mathcal{E}_\mathrm{lo}(t)$, varies too quickly to be followed by the photodetectors, and we will only be able to measure integrals over the pulse duration. The terms to be related are thus:

$$\mathcal{E}_\mathrm{lo}^*\hat{a} \Longleftrightarrow \int \mathrm{d}t\, \mathcal{E}_\mathrm{lo}^*(t)\hat{E}(t) = 2\pi\int \mathrm{d}\omega\, \mathcal{E}_\mathrm{lo}^*[\omega]\hat{a}_\omega, \tag{7}$$

where $\hat{a}$ is the mixed field defined in equation (1).

The observables $\hat{\imath}$ and $\hat{I}$ of the current in the output port of these homodyne detectors are then

$$\hat{\imath} = \mathcal{E}_\mathrm{lo}^*\hat{a} + \mathcal{E}_\mathrm{lo}\hat{a}^\dagger \Longleftrightarrow \hat{I} = 2\pi\left(\int \mathrm{d}\omega\, \mathcal{E}_\mathrm{lo}^*[\omega]\hat{a}_\omega + \int \mathrm{d}\omega\, \mathcal{E}_\mathrm{lo}[\omega]\hat{a}_\omega^\dagger\right). \tag{8}$$

2.3 Correspondence between the imperfect monomode and the perfect pulsed homodyne detectors

2.3.1 Moment operators

We want the observables $\hat{\imath}$ and $\hat{I}$ to have the same probability distribution. We therefore need to have the same moments $\langle\hat{I}^p\rangle$ and $\langle\hat{\imath}^p\rangle$ for every integer p. This condition is sufficient because the equality of the Fourier transforms $\langle\mathrm{e}^{\mathrm{i}\Omega\hat{I}}\rangle$ and $\langle\mathrm{e}^{\mathrm{i}\Omega\hat{\imath}}\rangle$ of the probability distribution of the observables follows straightforwardly.

To find this pth moment for any n-photons Fock state and for both detectors, we can define "moment operators" $\tilde{\imath}_{p,n}$ and $\tilde{I}_{p,n}$ as follows:

$$\langle n|\hat{\imath}^p|n\rangle \equiv \langle 0|\tilde{\imath}_{p,n}|0\rangle \Longleftrightarrow \langle\psi_n|\hat{I}^p|\psi_n\rangle \equiv \langle 0|\tilde{I}_{p,n}|0\rangle \tag{9}$$

$$\tilde{\imath}_{p,n} = \frac{1}{n!}\hat{a}_\mathrm{s}^n\left[\mathcal{E}_\mathrm{lo}^*\hat{a} + \mathcal{E}_\mathrm{lo}\hat{a}^\dagger\right]^p\hat{a}_\mathrm{s}^{\dagger n} \Longleftrightarrow$$
$$\tilde{I}_{p,n} = \frac{[2\pi]^p}{n!}\hat{A}_\mathrm{s}^n\left[\int \mathrm{d}\omega\, \mathcal{E}_\mathrm{lo}^*[\omega]\hat{a}_\omega + \int \mathrm{d}\omega\, \mathcal{E}_\mathrm{lo}[\omega]\hat{a}_\omega^\dagger\right]^p\hat{A}_\mathrm{s}^{\dagger n}. \tag{10}$$

The bracketed expressions should be expanded to calculate the mean-value of these operators in vacuum. This development should be the same for both homodyne detectors, up to the analogy (7). In order to simplify the calculations of the average values, the annihilation and creation operators can be rewritten in normal order. The two results will be easily related by comparison of the multiplicative coefficients.

2.3.2 Commutators

In order to rewrite the above expressions in normal order without writing explicitly all terms, it is actually enough to realize that they can be obtained from the following commutators:

$$\left[\mathcal{E}_\mathrm{lo}^*\hat{a}, \mathcal{E}_\mathrm{lo}\hat{a}^\dagger\right] = \mathcal{E}_\mathrm{lo}^*\mathcal{E}_\mathrm{lo} \Longleftrightarrow \left[2\pi\int \mathrm{d}\omega\, \mathcal{E}_\mathrm{lo}^*[\omega]\hat{a}_\omega, 2\pi\int \mathrm{d}\omega\, \mathcal{E}_\mathrm{lo}[\omega]\hat{a}_\omega^\dagger\right] = 2\pi\langle\mathcal{E}_\mathrm{lo}|\mathcal{E}_\mathrm{lo}\rangle \tag{11}$$

$$\left[\mathcal{E}_\mathrm{lo}^*\hat{a}, \hat{a}_\mathrm{s}^\dagger\right] = \mathcal{E}_\mathrm{lo}^*t \Longleftrightarrow \left[2\pi\int \mathrm{d}\omega\, \mathcal{E}_\mathrm{lo}^*[\omega]\hat{a}_\omega, \hat{A}_\mathrm{s}^\dagger\right] = \sqrt{2\pi}\frac{\langle\mathcal{E}_\mathrm{lo}|\xi\rangle}{\sqrt{\langle\xi|\xi\rangle}}\cdot \tag{12}$$

Because of the similarly of the precedent developments, similar commutators appear at the same place with the same coefficients in both developments.

We can thus link the parameters of the two kind of homodyne detectors discussed here using equations (11, 12):

$$\mathcal{E}_\mathrm{lo}^* t\, t^*\mathcal{E}_\mathrm{lo} \Longleftrightarrow 2\pi\frac{\langle\mathcal{E}_\mathrm{lo}|\xi\rangle\langle\xi|\mathcal{E}_\mathrm{lo}\rangle}{\langle\xi|\xi\rangle} \tag{13}$$

$$|t|^2 \equiv \eta \Longleftrightarrow \frac{\langle\mathcal{E}_\mathrm{lo}|\xi\rangle\langle\xi|\mathcal{E}_\mathrm{lo}\rangle}{\langle\mathcal{E}_\mathrm{lo}|\mathcal{E}_\mathrm{lo}\rangle\langle\xi|\xi\rangle} = \frac{|\langle\mathcal{E}_\mathrm{lo}|\xi\rangle|^2}{\langle\mathcal{E}_\mathrm{lo}|\mathcal{E}_\mathrm{lo}\rangle\langle\xi|\xi\rangle} \tag{14}$$

$$t \Longleftrightarrow \frac{\langle\mathcal{E}_\mathrm{lo}|\xi\rangle}{\sqrt{\langle\mathcal{E}_\mathrm{lo}|\mathcal{E}_\mathrm{lo}\rangle\langle\xi|\xi\rangle}}\cdot \tag{15}$$

These expressions show us how to find the parameters of an imperfect monomode homodyne detector in order

to have the same moment operator development than a given pulsed homodyne detector, *i.e.*

$$|\mathcal{E}_{\rm lo}|^2 = 2\pi\langle\mathcal{E}_{\rm lo}^*|\mathcal{E}_{\rm lo}\rangle \qquad \text{[Eq. (11)]}$$
$$\text{and } \eta = \frac{|\langle\mathcal{E}_{\rm lo}|\xi\rangle|^2}{\langle\mathcal{E}_{\rm lo}|\mathcal{E}_{\rm lo}\rangle\langle\xi|\xi\rangle} \qquad \text{[Eq. (14)]}$$
$$\text{(or } t = \frac{\langle\mathcal{E}_{\rm lo}|\xi\rangle}{\sqrt{\langle\mathcal{E}_{\rm lo}|\mathcal{E}_{\rm lo}\rangle\langle\xi|\xi\rangle}} \text{ [Eq. (15)]).}$$

2.3.3 Calculation of the average value

If the substitutions discussed in the precedent paragraph are made, we have two strictly analog normal order operator development. Their mean value in the vacuum will only have terms like

$$[\mathcal{E}_{\rm lo}^*\hat{a}]^k\,[\hat{a}_{\rm s}]^l\,|0\rangle = \delta_{k,0}\,\delta_{l,0}|0\rangle \Longleftrightarrow \left[2\pi\int {\rm d}\omega\,\mathcal{E}_{\rm lo}^*[\omega]\hat{a}_\omega\right]^k\left[\hat{A}_{\rm s}\right]^l|0\rangle = \delta_{k,0}\,\delta_{l,0}|0\rangle \quad (16)$$

and their hermitian conjugate. Since these last analog terms are equal and preceded by identical complex coefficients, both mean values are equal:

$$\langle 0|\tilde{\imath}_{p,n}|0\rangle = \langle 0|\tilde{I}_{p,n}|0\rangle \;\; i.e. \;\; \langle n|\hat{\imath}^p|n\rangle = \langle\psi_n|\hat{I}^p|\psi_n\rangle, \quad (17)$$

for every integer p.

Since all their moments are equal, the two probability distributions are identical: a pulsed homodyne detector measuring a n-photons wave-packet is equivalent to a monomode imperfect homodyne detector measuring a n-photons Fock state with an efficiency given by

$$\eta_{\rm eff} = \frac{|\langle\mathcal{E}_{\rm lo}|\xi\rangle|^2}{\langle\mathcal{E}_{\rm lo}|\mathcal{E}_{\rm lo}\rangle\langle\xi|\xi\rangle}, \quad (18)$$

corresponding to a temporal mode-matching between the local-oscillator envelope and the wave-packet shape.

2.4 Generalization

2.4.1 Other quantum states

If the measured state is not a Fock state but a linear combination of the $|\psi_n\rangle$'s, the equivalence between the two kind of homodyne detectors holds on since $\eta_{\rm eff}$ is not n-dependent. It also holds for non-coherent combinations of such pure states.

However, the wave-packet shape ξ gives the value of $\eta_{\rm eff}$. Therefore, homodyne measurement of a coherent superposition of diversely shaped wave packets is more complicated to describe, because several temporal modes are involved and will not be considered here.

2.4.2 Non-perfect pulsed homodyne detector

Beyond the time-frequency aspects which were considered up to now, homodyne detectors have usually various other defects, related to non-perfect detector efficiency, imperfect wave-front matching... These imperfections can be modelized by introducing losses from a fictitious beam splitter, in the same way as as for monomode homodyne detectors. The measured field is then $\hat{A} = \tau\hat{A}_{\rm s} + \rho\hat{A}_{\rm N}$, where $|\tau| = \sqrt{\eta_{\rm loss}}$, and $|\tau|^2 + |\rho|^2 = 1$. The relevant commutator relation is then

$$\left[\frac{1}{2\pi}\int {\rm d}\omega\,\mathcal{E}_{\rm lo}^*[\omega]\hat{a}_\omega, \hat{A}^\dagger\right] = \tau^*\left[\frac{1}{2\pi}\int {\rm d}\omega\,\mathcal{E}_{\rm lo}^*[\omega]\hat{a}_\omega, \hat{A}_{\rm s}^\dagger\right] \quad (19)$$

and the total efficiency $\eta_{\rm tot}$ becomes

$$\eta_{\rm tot} = |\tau|^2\frac{|\langle\mathcal{E}_{\rm lo}|\xi\rangle|^2}{\langle\mathcal{E}_{\rm lo}|\mathcal{E}_{\rm lo}\rangle\langle\xi|\xi\rangle} = \eta_{\rm loss}\eta_{\rm eff}. \quad (20)$$

The effective total efficiency of an imperfect pulsed homodyne detector is thus the product of the loss induced efficiency and the pulse-induced effective efficiency.

3 Evaluations of the effective quantum efficiency

3.1 Continuous experiment

Yurke and Stoler [7] proposed to measure the probability distribution of a single-photon using continuously pumped parametric down-conversion medium and a gated homodyne detector. The input channel is opened for a duration δT only when a photon in the idler beam is detected. This is equivalent to a square-pulsed homodyne detector with a local oscillator field envelope defined by

$$\mathcal{E}_{\rm lo}(t) = \begin{cases} \dfrac{1}{\sqrt{\delta T}} & \text{if } |t| < \dfrac{\delta T}{2} \\ 0 & \text{if } |t| \geq \dfrac{\delta T}{2} \end{cases} \quad (21)$$

where $\mathcal{E}_{\rm lo}$ is normalized according to $\langle\mathcal{E}_{\rm lo}|\mathcal{E}_{\rm lo}\rangle = \int {\rm d}t\,|\mathcal{E}_{\rm lo}|^2 = 1$. The idler photon frequency ω_i is selected with a monochromator of width $\delta\omega_{\rm i}$ (see Fig. 3). In this scheme the pump and the local oscillator are initially c.w. lasers, and their linewidths are supposed small compared to the spectral widths $\delta\omega_{\rm i}$ and $1/\delta T$. On the other hand, the phase matching bandwidth of the non-linear crystal is assumed to be very broad compared to the same spectral widths. Since the down-conversion process fulfills the energy conservation relation $\omega_{\rm s} + \omega_{\rm i} = \omega_{\rm p}$, where $\omega_{\rm p}$ is the pump frequency, and $\omega_{\rm s}$, $\omega_{\rm i}$ are the signal and idler frequencies, $\omega_{\rm s}$ will be defined with the same precision as $\omega_{\rm i}$, and one has $\delta\omega_{\rm s} = \delta\omega_{\rm i}$. The signal wave packet in the frequency domain is thus:

$$\xi[\omega_{\rm s}] = \begin{cases} \dfrac{1}{\sqrt{2\pi\,\delta\omega_{\rm i}}} & \text{if } |\omega_{\rm s}| < \dfrac{\delta\omega_{\rm i}}{2} \\ 0 & \text{if } |\omega_{\rm s}| \geq \dfrac{\delta\omega_{\rm i}}{2}, \end{cases} \quad (22)$$

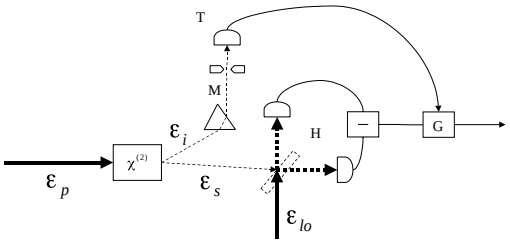

Fig. 3. Single-photon field measurement. The two correlated beams $\mathcal{E}_\mathrm{i}$ and $\mathcal{E}_\mathrm{s}$ are produced by parametric-down conversion of the pump-beam $\mathcal{E}_\mathrm{p}$ in a $\chi^{(2)}$ non-linear medium. The detection of a photon in the idler-beam $\mathcal{E}_\mathrm{i}$ by the avalanche photodiode (or photomultiplier) T triggers the gate G and thus the measurement of the signal-beam $\mathcal{E}_\mathrm{s}$ by the homodyne detector H. The role of the monochromator M is discussed in the text.

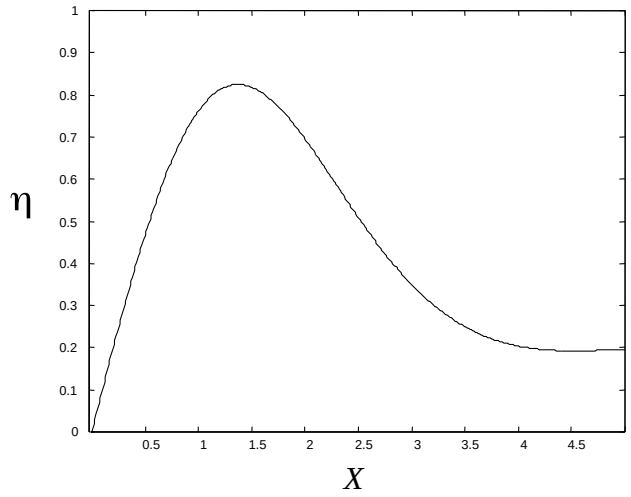

Fig. 4. Effective quantum efficiency $\eta_\mathrm{eff}(X)$ for a "chopped" continuous experiment. The value of $\eta_\mathrm{eff}(X)$ obtained from equation (23) is plotted as a function of $X = \delta\omega_\mathrm{i}\,\delta T/2\pi$.

and is also normalized according to $\langle\xi|\xi\rangle = 2\pi\int \mathrm{d}\omega\,|\xi[\omega]|^2 = 1$.

The best achievable efficiency η_opt can then be obtained by calculating the scalar product $\langle\xi|\mathcal{E}_\mathrm{lo}\rangle$. It is convenient to define the new variables $x = \omega\,\delta T/2\pi$ and $X = \delta\omega_\mathrm{i}\,\delta T/2\pi$. The effective efficiency $\eta_\mathrm{eff}(X)$ is then easy to compute, since $\mathcal{E}_\mathrm{lo}$ and ξ are normalized, and we obtain:

$$\eta_\mathrm{eff}(X) = \frac{1}{X}\left|\int_{-\frac{X}{2}}^{\frac{X}{2}} \mathrm{d}x\,\mathrm{sinc}\,(\pi x)\right|^2 = \frac{4}{X}\left|\int_{0}^{\frac{X}{2}} \mathrm{d}x\,\mathrm{sinc}\,(\pi x)\right|^2. \tag{23}$$

The behaviour of this quantity is shown in Figure 4. Numerical calculations shows that the optimal value of $\eta_\mathrm{eff}(X)$ is $\eta_\mathrm{opt} = 82.5\%$, when $X = 1.37$. Even a perfect homodyne detector with an optimal pulse duration has 17.5% extra-losses in a continuous regime.

In order to evaluate some orders of magnitude, one may consider filtering the idler with a good grating monochromator or interference filter, which gives $\delta\lambda = 0.1$ nm. The linewidth and time window are then $\delta\omega_\mathrm{i} = 2\pi c\delta\lambda/\lambda^2$ and $\delta T = 2\pi X/\delta\omega_\mathrm{i} = X\lambda^2/c\,\delta\lambda$. With near infrared photons ($\lambda = 1\ \mu$m) the optimal gate duration for $\delta\lambda = 0.1$ nm is $\delta T_\mathrm{opt} = 45$ ps. This time is too small to be obtained by using an electronic gate. One might thus use narrower filters, based on Fabry-Perot resonators, but in any case the present scheme will be limited by the rather stringent matching which is required between $\delta\omega_\mathrm{i}$ and δT. We will see now that the required condition is much easier to fulfill by using a pulsed local oscillator.

3.2 Pulsed experiment

3.2.1 General features

In the pulsed regime, it is possible to use pump pulses short enough, so that their linewith $\delta\omega_\mathrm{p}$ becomes greater than the monochromator linewidth $\delta\omega_\mathrm{i}$. Then the energy conservation relation $\omega_\mathrm{p} = \omega_\mathrm{i} + \omega_\mathrm{s}$ yields $\delta\omega_\mathrm{s} = \delta\omega_\mathrm{p}$. If the pump pulses are frequency-doubled local-oscillator pulses, the photon wavepacket and the L.O. will have approximately the same linewidth, and it will be much easier to get a good overlap between them. Another advantage of a pulsed scheme is that the arrival time window of the wave-packet is known, which allows one to discard many "dark counts" of the triggerring photon counter. A pulsed experiment has thus no fundamental limitation of the effective efficiency η_eff since the measured wave-paket and the local oscillator envelope could overlap perfectly.

In order to evaluate explicitly the single photon wavepacket, we will describe here the quantum state of the correlated beams i and s out of the nonlinear medium. If the $\chi^{(2)}$ medium is pumped with a field $E_\mathrm{p}(t) = \mathcal{E}_\mathrm{p}(t)\mathrm{e}^{-2\mathrm{i}\omega_0 t}$, the interaction hamiltonian in the crystal is:

$$\hat{H}(t) = \hbar\mathcal{E}_\mathrm{p}(t)\mathrm{e}^{-2\mathrm{i}\omega_0 t}\hat{E}_\mathrm{s}^\dagger(t)\hat{E}_\mathrm{i}^\dagger(t) + \mathrm{H.C.} \tag{24}$$

$$= \hbar\mathcal{E}_\mathrm{p}(t)\int \mathrm{d}\omega\mathrm{d}\omega'\mathrm{e}^{\mathrm{i}(\omega+\omega'-2\omega_0)t}\hat{a}_{\mathrm{s}\omega}^\dagger\hat{a}_{\mathrm{i}\omega'}^\dagger + \mathrm{H.C.}, \tag{25}$$

where the $\chi^{(2)}$ coefficient is "hidden" in the pump enveloppe. At the first order of a perturbation theory, and assuming very large phase-matching bandwidth and very small group velocity dispersion and mismatch, the field state is

$$|\psi(t)\rangle \simeq \left[1 + \frac{1}{\mathrm{i}\hbar}\int_0^t \mathrm{d}t'\hat{H}(t')\right]|0\rangle \tag{26}$$

$$\simeq |0\rangle - \mathrm{i}\int \mathrm{d}\omega\mathrm{d}\omega'\,|s,\omega{:}1\rangle \otimes|i,\omega'{:}1\rangle\int_0^t \mathrm{d}t'\,\mathcal{E}_\mathrm{p}(t')\mathrm{e}^{\mathrm{i}(\omega+\omega'-2\omega_0)t'}. \tag{27}$$

If the idler-monochromator is narrower than the pulse linewidth, and centered in the L.O. frequency ω_0, the field state is projected onto $|i,\omega_0{:}1\rangle$ when a photon is detected in the monochromated idler beam, and the field

state becomes

$$|\psi_{\rm s}(t)\rangle = \alpha\langle {\rm i},\omega_0{:}1|\psi(t)\rangle \tag{28}$$

$$\simeq -{\rm i}\alpha\int {\rm d}\omega\,|s,\omega{:}1\rangle\int_0^t {\rm d}t'\,\mathcal{E}_{\rm p}(t'){\rm e}^{{\rm i}(\omega-\omega_0)t'} \tag{29}$$

where α is a normalization coefficient. In practice, we will be interested in the field state after the pump went through the crystal. If the group velocity mismatch is small enough and the crystal long enough, this corresponds to taking the limit of very large t in the above equation, and the final field state can be written:

$$|\psi_{\rm s}\rangle \simeq -\frac{\rm i}{\sqrt{2\pi\langle\mathcal{E}_{\rm p}|\mathcal{E}_{\rm p}\rangle}}\int {\rm d}\omega\,\mathcal{E}_{\rm p}[\omega_0-\omega]|s,\omega{:}1\rangle. \tag{30}$$

The photon wave-packet has therefore the same width as the pump envelope:

$$\xi[\omega] = \alpha\mathcal{E}_{\rm p}[\omega_0-\omega]. \tag{31}$$

In a real non-linear medium, one has to take the group velocity mismatch and the group velocity dispersion into account. The first one increases the generated photon wave packet duration and the latter induces a frequency chirp. One should also not forget the finiteness of the nonlinear crystal, that broaden the phase-matching condition and the wave-packet spectral width. These effects can be included in the expression of ξ, changing the scalar product $\langle\xi|\mathcal{E}_{\rm lo}\rangle$ and the effective efficiency $\eta_{\rm eff}$ of the homodyne detection.

3.2.2 Explicit calculations for Gaussian pulses

For an explicit result, we assume that the local-oscillator pulse envelope $\mathcal{E}_{\rm lo}(t)$ is Gaussian-shaped, and that the pump field is the frequency-doubled local-oscillator. The phase-matching bandwidth is assumed to be much larger than the pulses bandwidths, and the two envelopes are normalized according to $\langle\mathcal{E}_{\rm lo}|\mathcal{E}_{\rm lo}\rangle = \langle\mathcal{E}_{\rm p}|\mathcal{E}_{\rm p}\rangle = 1$. The pulse shapes are thus

$$\mathcal{E}_{\rm lo}(t) = \frac{2^{\frac{1}{4}}}{\sqrt{\delta T}\,\pi^{\frac{1}{4}}}\,{\rm e}^{-\frac{t^2}{\delta T^2}}$$

$$\text{and}\quad \mathcal{E}_{\rm p}(t) = \alpha\mathcal{E}_{\rm lo}^2(t) = \frac{\sqrt{2}}{\sqrt{\delta T}\,\pi^{\frac{1}{4}}}\,{\rm e}^{-\frac{2t^2}{\delta T^2}}. \tag{32}$$

We obtain then, using equation (31),

$$\langle\mathcal{E}_{\rm lo}|\xi\rangle = \langle\mathcal{E}_{\rm lo}|\mathcal{E}_{\rm p}\rangle = \frac{2^{\frac{3}{4}}}{\delta T\sqrt{\pi}}\int {\rm d}t\,{\rm e}^{-\frac{3t^2}{\delta T^2}} = \frac{2^{\frac{3}{4}}}{\sqrt{3}} \tag{33}$$

and

$$\eta_{\rm eff} = \frac{|\langle\mathcal{E}_{\rm lo}|\xi\rangle|^2}{\langle\mathcal{E}_{\rm lo}|\mathcal{E}_{\rm lo}\rangle\langle\xi|\xi\rangle} = \frac{2\sqrt{2}}{3} \simeq 94.3\%. \tag{34}$$

This effective efficiency is very high, but holds only for Gaussian pulses, without any dispersive effect of the nonlinear medium.

For these calculations to be valid, the monochromator linewidth $\delta\lambda_{\rm i}$ should be smaller than the signal wave-packet linewidth. Using the same conditions as in the previous section ($\lambda_{\rm s} = 1$ μm, $\delta\lambda_{\rm i} = 0.1$ nm), we obtain $\delta T_{\rm p} \ll 30$ ps. We need therefore to be in the subpicosecond (or few picoseconds) regime.

3.2.3 More general idler-monochromator

The above calculations can be easily generalized to include a finite linewidth $\delta\omega_{\rm i}$ of the monochromator. The field state is then projected onto $\int_{-\frac{\delta\omega_{\rm i}}{2}}^{\frac{\delta\omega_{\rm i}}{2}} {\rm d}\delta\omega|i,\omega_0+\delta\omega{:}1\rangle$, and:

$$|\psi_{\rm s}(t)\rangle = \alpha\int_{-\frac{\delta\omega_{\rm i}}{2}}^{\frac{\delta\omega_{\rm i}}{2}} {\rm d}\delta\omega\langle i,\omega_0+\delta\omega{:}1|\psi(t)\rangle \tag{35}$$

$$\simeq -{\rm i}\alpha\int {\rm d}\omega\,|s,\omega{:}1\rangle\int_0^t {\rm d}t'\,\mathcal{E}_{\rm p}(t') \times\int_{-\frac{\delta\omega_{\rm i}}{2}}^{\frac{\delta\omega_{\rm i}}{2}} {\rm d}\delta\omega\,{\rm e}^{{\rm i}(\omega-\omega_0+\delta\omega)t'}. \tag{36}$$

Taking again the long-time limit for t, the quantum state is

$$|\psi_{\rm s}\rangle \simeq -{\rm i}\alpha\int {\rm d}\omega\int_{-\frac{\delta\omega_{\rm i}}{2}}^{\frac{\delta\omega_{\rm i}}{2}} {\rm d}\delta\omega\,\mathcal{E}_{\rm p}[\omega_0-\omega-\delta\omega]|s,\omega{:}1\rangle \tag{37}$$

and

$$\xi[\omega] \simeq -{\rm i}\alpha\int_{-\frac{\delta\omega_{\rm i}}{2}}^{\frac{\delta\omega_{\rm i}}{2}} {\rm d}\delta\omega\,\mathcal{E}_{\rm p}[\omega_0-\omega-\delta\omega]. \tag{38}$$

The calculations can again be carried out explicitly for Gaussian pulses, and by using the variables $x = \delta\omega\,\delta T/2\pi$ and $X = \delta\omega_{\rm i}\,\delta T/2\pi$ as previously, one obtains:

$$\langle\mathcal{E}_{\rm lo}|\xi\rangle = \frac{-2^{\frac{3}{4}}{\rm i}}{\sqrt{3}\,X}\int_{-\frac{X}{2}}^{\frac{X}{2}} {\rm d}x\,{\rm e}^{-\frac{\pi^2x^2}{3}}. \tag{39}$$

Since $\mathcal{E}_{\rm lo}$ and ξ are normalized, the effective efficiency is thus

$$\eta_{\rm eff}(X) = \frac{2\sqrt{2}}{3X^2}\left|\int_{-\frac{X}{2}}^{\frac{X}{2}} {\rm d}x\,{\rm e}^{-\frac{\pi^2x^2}{3}}\right|^2 = \frac{8\sqrt{2}}{3X^2}\left|\int_0^{\frac{X}{2}} {\rm d}x\,{\rm e}^{-\frac{\pi^2x^2}{3}}\right|^2. \tag{40}$$

The behaviour of this quantity is now shown in Figure 5. Numerical calculations shows that $\eta_{\rm eff} > 90\%$ for $X < 0.29$ and $\eta_{\rm eff} > 50\%$ for $X < 1.16$. Since $\delta T = X\lambda^2/c\,\delta\lambda$ the pulse duration needed to have a given effective efficiency can be calculated easily. With near infrared photons ($\lambda = 1$ μm) and a monochromator resolution $\delta\lambda = 0.1$ nm, this pulse duration is $\delta T_{90} \approx 10$ ps for a 90% effective efficiency and $\delta T_{50} \approx 40$ ps for 50% efficiency. Obviously shorter (or longer) values will be obtained by broadening (or narrowing) the filtering linewidth.

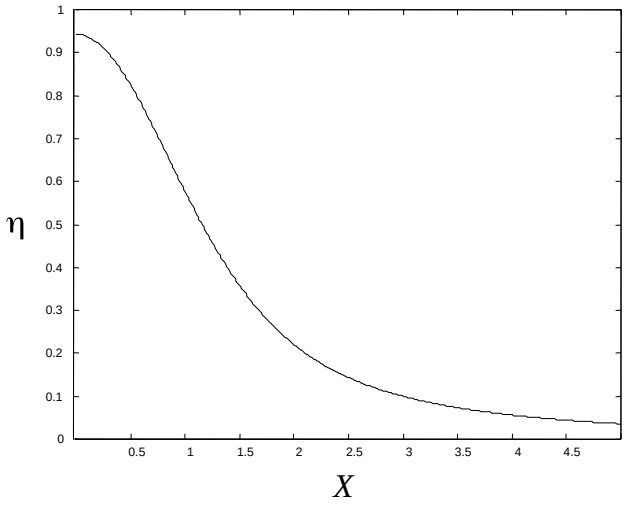

Fig. 5. Effective quantum efficiency $\eta_{\rm eff}(X)$ for a pulsed experiment with Gaussian-shaped pulses. The value of $\eta_{\rm eff}(X)$ obtained from equation (40) is plotted as a function of $X = \delta\omega_{\rm i}\ \delta T/2\pi$.

4 Conclusion

In order to describe the homodyne detection of conditional single photon state, we have defined an "effective quantum efficiency" which appears as the normalized scalar product of the single photon and local oscillator wavepackets. We have shown that this effective quantum efficiency is a useful tool to evaluate and compare various experimental possibilities which are under consideration for realizing pulsed homodyne detection experiments.

This work was carried out in the framework of the european IST/FET/QIPC project "QUICOV".

References

1. See quantum optics textbooks, *e.g.* R. Loudon, *The Quantum Theory of Light*, (Clarendon Press, Oxford, 1983); or C. Cohen-Tannoudji, J. Dupont-Roc, G. Grynberg, *Atom-photon interaction. Basic Processes and Applications* (Wiley, New-York, 1992).
2. C.K. Hong, L. Mandel, Phys. Rev. Lett. **56**, 58 (1986).
3. P. Grangier, G. Roger, A. Aspect, Europhys. Lett. **1**, 173 (1986).
4. For a review see W. Tittel, G. Ribordy, N. Gisin, Physics World, p. 41, march 1998.
5. H.J. Kimble, M. Dagenais, L. Mandel, Phys. Rev. Lett. **39**, 691 (1977).
6. F. Diedrich, H. Walther, Phys. Rev. Lett. **58**, 203 (1987).
7. B. Yurke, D. Stoler, Phys. Rev. A **36**, 1955 (1987).
8. S. Schiller *et al.,* Communication at the conference *Quantum Communication, Measurement and Computing*, Capri, Italy, July 2000.
9. Z.Y. Ou, Quant. Semiclass. Opt. **9**, 599 (1997).
10. C. Cohen-Tannoudji, B. Diu, F. Laloë, *Quantum Mechanics*, complement B_V (Wiley, New-York, 1992).